Rare Metal Materials and Engineering
Volume 50, Issue 9, September 2021
Available online at www.rmme.ac.cn

Science Press

Cite this article as: Chen Xiao, Li Chengdi, Zhou Hongkai, et al. Microstructure and Properties of In Situ Synthesized MoB/NiCr Coatings with Different (Mo+B)/(Ni+Cr) Mass Ratios[J]. Rare Metal Materials and Engineering, 2021, 50(09): 3085-3093.

ARTICLE

Microstructure and Properties of In Situ Synthesized MoB/NiCr Coatings with Different (Mo+B)/(Ni+Cr) Mass Ratios

Chen Xiao[1,3], Li Chengdi[1,2], Zhou Hongkai[1], Pi Zhimin[1], Bai Xiaobo[3]

[1] Xinyu Key Laboratory of Materials Technology and Application for Intelligent Manufacturing, Xinyu University, Xinyu 338004, China; [2] National Center for International Research of Subsea Engineering Technology and Equipment, Dalian Maritime University, Dalian 116026, China; [3] Jiangxi Province Engineering Research Center of Materials Surface Enhancing & Remanufacturing, Jiujiang University, Jiujiang 332005, China

Abstract: Three kinds of Mo-B-Ni-Cr ball-milled mixture powders with different (Mo+B)/(Ni+Cr) mass ratios (1∶1, 2∶1, and 3∶1) were deposited by the high velocity oxygen-fuel (HVOF) spraying process to in situ synthesize MoB/NiCr coatings. The microstructure and phase composition of MoB/NiCr coatings were analyzed by scanning electron microscope (SEM) and X-ray diffraction (XRD). The effects of different (Mo+B)/(Ni+Cr) mass ratios on the microstructure, microhardness, bonding strength, and corrosion resistance of MoB/NiCr coatings were discussed. The results show that MoB/NiCr coatings with (Mo+B)/(Ni+Cr) mass ratio of 1∶1 have the lowest porosity and the largest thickness. Mo_2NiB_2 ternary boride was in situ synthesized in all three kinds of MoB/NiCr coatings. The content of Mo_2NiB_2 ternary boride is increased with increasing the (Mo+B)/(Ni+Cr) mass ratio. The microhardness of MoB/NiCr coatings is increased with increasing the (Mo+B)/(Ni+Cr) mass ratio, while the bonding strength is decreased. After immersion test in molten zinc for 360 h, no zinc or its intermetallic compound can be observed in the surface region of MoB/NiCr coatings according to energy disperse spectrometer (EDS) and XRD analyses. The porosity of the coatings is increased with increasing the (Mo+B)/(Ni+Cr) mass ratio, while the thickness is decreased. Compared with other coatings, the MoB/NiCr coating with (Mo+B)/(Ni+Cr) mass ratio of 1:1 has better corrosion resistance in molten zinc.

Key words: Mo_2NiB_2 ternary boride; high velocity oxygen-fuel; microstructure; microhardness; corrosion resistance

Due to the corrosion behavior of the metal in liquid zinc bath, prolonging service life of metal components in hot-dip galvanizing industry is an urgent problem[1-4]. Currently, the coating materials (WC-based cermets, intermetallic compounds, ceramics) deposited on the surface of metal components by thermal spraying processes are commonly used for improving corrosion resistance in the industrial galvanizing bath[5]. Mizuno et al[6] revealed that WC-12wt% Co coating with lower carbon content shows higher durability in the Al-45wt% Zn bath. However, the reaction layer composed of Al, Zn, W, and Co was observed on the coating surface, and cracks were easily generated in the reaction layer. Seong et al[7] reported that WC-12wt% Co coating is sprayed on the roll surface to improve the corrosion resistance. However, the molten zinc or aluminum penetrates the micro-cracks generated in the WC-12wt% Co coating, and Al-Fe-Zn layers are formed on the coating surface. Zhang et al[8] reported that big cracks and more fragments are peeled off from the corners of WC-12wt% Co coating after 300 times of thermal shock cycle tests, and zinc atoms diffuse along the cracks into the WC-12wt% Co coating after immersion for 360 h in molten zinc. Xie et al[9] revealed that due to large difference in coefficient of thermal expansion (CTE) between FeB-12wt% $Al_{0.25}$FeNiCoCr coating deposited by active combustion high velocity air-fuel (AC-HVAF) process and the substrate, the penetration of liquid zinc into the cracks caused by residual stress leads to the failure of the coating. Dong et al[10] reported that due to the lower porosity and residual stress of ZrO_2-Ni/Al gradient coatings sprayed by plasma spraying, the average lifetime of gradient coatings is 4 times as long as that

Received date: September 06, 2020
Foundation item: National Natural Science Foundation of China (51861012); Science and Technology Project of Jiangxi Educational Bureau (GJJ191068, GJJ191049); Science Technology Project of Jiujiang City ([2015]-64)
Corresponding author: Li Chengdi, Ph. D., National Center for International Research of Subsea Engineering Technology and Equipment, Dalian Maritime University, Dalian 116026, P. R. China, Tel: 0086-411-84729228, E-mail: cdl1988_xyxy@126.com

of general ZrO_2 coatings. However, due to the existence of pseudo-connected pores in the ZrO_2 ceramic top layer, zinc atoms could penetrate through the ZrO_2 coating and react with Ni/Al bond layer. Yan et al[11] also reported that compared with Fe_2Al_5 and $FeAl_2$ intermetallic compounds, FeAl has higher corrosion resistance to liquid zinc. However, FeAl coating is still corroded by molten zinc. Oxide ceramic materials (Al_2O_3, ZrO_2, Y_2O_3) are usually used as corrosion-resistant coating materials owing to their stable properties. Therefore, Al_2O_3 and ZrO_2-8wt% Y_2O_3 coatings are prepared by plasma spraying to protect the substrate in the molten Al-45wt% Zn[6]. It is revealed that the lifetime of spray-coated specimens is longer than that of the substrate. Since CTE of ZrO_2-8wt% Y_2O_3 coating is closer to that of the substrate, the lifetime of ZrO_2-8wt% Y_2O_3 coating is longer than that of Al_2O_3 coating. However, the cracks are easily generated in the ceramic coatings during heat-shock resistance tests, leading to the decrease of durability of ceramic coating. Therefore, it is urgent to find a novel coating material applied to galvanizing industry.

Boride cermet coating material with excellent properties (corrosion, wear, and oxidation resistance) has been applied in galvanizing industry[12,13]. MoB-based cermet coating composed of ternary borides (Mo_2FeB_2, Mo_2CoB_2, MoCoB, and Mo_2NiB_2) as novel coating materials has been widely studied. Wei et al[14] reported that the microstructural morphology of Mo_2FeB_2-based cermet coating deposited by electrospark deposition (ESD) process is dense, and the interface between the coating and substrate shows metallurgical bonding. However, the stress relief cracks can be induced owing to the large temperature gradients and the poor ductility of the coating. Mizuno et al[6] reported that MoB/CoCr coating composed of Mo_2CoB_2 and MoCoB ternary borides has much higher durability. However, due to the large difference of CTE between MoB/CoCr coating (9.2×10^{-6} K^{-1}) and AISI316L substrate (19.3×10^{-6} K^{-1}), the cracks are obviously generated in the coating after immersion test, even the undercoating is sprayed between MoB/CoCr coating and the substrate. Dong et al[10] reported that MoB/CoCr coating has higher durability than WC-12wt% Co coating does. However, the molten zinc can penetrate the vertical cracks induced by residual stress to corrode the substrate. MoB-CoCr alloy coating has strong interfacial bond strength and excellent mechanical properties[15,16], and the thickness of MoB-based cermet coatings with NiCr bond coating after the immersion test is similar to that of the as-sprayed coating[17]. Meanwhile, it also reveals that MoB-NiCr coating shows better mechanical property and durability than MoB/CoCr, NiCr, and CoMoCr coatings do[17].

Although certain as-sprayed coatings were studied for corrosion resistance in galvanizing industry, some main deficiencies (large CTE difference between the coating and substrate, stress cracks in the coating, high porosity, especially the expensive cost of MoB/CoCr and MoB/NiCr raw materials) restrict their industry application. Meanwhile, the effects of (Mo+B)/(Ni+Cr) mass ratio on the microstructure and properties of the coatings are rarely reported. Therefore, in order to reduce the manufacturing cost and analyze the effect of (Mo+B)/(Ni+Cr) mass ratio on the microstructure and properties of the coatings, MoB/NiCr coatings composed of Mo-Ni-B ternary boride were in situ synthesized by high velocity oxygen-fuel (HVOF) spraying process in this study.

1 Experiment

316L stainless-steel with dimensions of 50 mm×25 mm×3 mm was used as the substrate, which was cut into rectangular plates for the microstructure observation, mechanical property tests, and erosion evaluation of coatings. Prior to thermal spraying, the plates were pre-cleaned by acetone for 10 min in ultrasonic cleaner, and then grit blasted by aluminum oxide of 700 μm to achieve a roughened surface for improving the bonding strength between the coating and substrate. Raw materials of top coating in this study were Mo, B, Ni, and Cr. Co-based alloy spherical powder (29.0wt% Cr, 4.0wt% W, 3.0wt% Ni, 3.0wt% Fe, 1.1wt% Si, 1.0wt% Mo, and balanced Co) was used as raw material of the bond coating. The morphologies of the powders are shown in Fig.1. The preparation process of Mo-B-Ni-Cr mixture powders is as follows. Firstly, Mo, B, Ni, and Cr powders were wet-milled by a planetary ball mill (QM-QX4). The rotation speed, milling time, and ball-to-powder mass ratio were 200 r/min, 3 h, and 10:1, respectively. Anhydrous ethanol was used as a milling medium. Secondly, the milled powders were stirred by a constant-temperature magnetic stirrer (SG-5411) at a rotation speed of 150 r/min and water temperature of 95 °C, and polyvinyl alcohol (PVA) binder was simultaneously added to agglomerate the milled powders. Thirdly, the mixture powders with PVA binder after stirring were put into general electric blast drying oven (DHG-9055A) for 6 h. Finally, the dried mixture powders were crushed in the mortar to obtain thermal spraying Mo-B-Ni-Cr mixture particles. Three types of specimens in Mo-B-Ni-Cr mixture powders were prepared according to different mass ratios of (Mo+B)/(Ni+Cr) of 1:1, 2:1, and 3:1. Meanwhile, the atomic ratio of Mo to B was 1:1, and that of Ni to Cr was also 1:1. A designed HVOF spray system (CH-2000, developed at Xi'an Jiaotong University, Xi'an, China) was used to deposit Mo-B-Ni-Cr mixture powders. The spraying parameters of MoB/NiCr and Co-based alloy bond coatings are listed in Table 1.

Microhardness measurements of MoB/NiCr coatings, Co-based bond coating, and 316L stainless-steel substrate were performed using HXD-1000 microhardness tester under load of 300 g for 20 s. The mean microhardness was obtained from the polished cross-sections of random 10 indents. According to ASTM C633-79 standard method, the bond strength testing was conducted on a standard tensile tester (TY 8000). The bond strength of MoB/NiCr coatings was obtained from the average value of three testing results. The surface roughness of Co-based alloy bond coating and the substrate was measured using a TA620-A surface roughness instrument. The average porosity, thickness, and ternary boride content of MoB/NiCr coatings were calculated by the image analysis

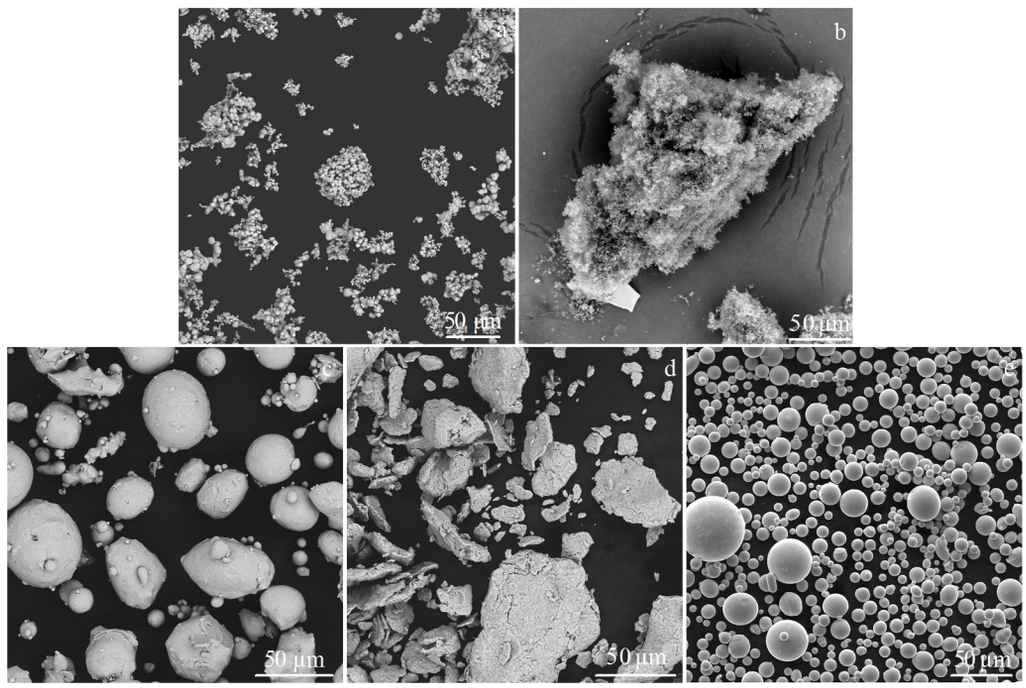

Fig.1 Morphologies of Mo (a), B (b), Ni (c), and Cr (d) powders and Co-based alloy (e)

Table 1 Spraying parameters of MoB/NiCr and Co-based alloy coatings

Spray parameter	MoB/NiCr	Co-based alloy
Oxygen flow rate/L·min^{-1}	402	322
Fuel (propane) flow rate/L·min^{-1}	36	24
Carrier gas (nitrogen) flow rate/L·min^{-1}	45	45
Powder feed rate/r·min^{-1}	50	30
Standoff distance/mm	200	160
Oxygen pressure/MPa	0.6	0.6
Fuel (propane) pressure/MPa	0.4	0.4
Carrier gas (nitrogen)/MPa	0.55	0.55

method (Software Image J) through scanning electron microscope (SEM) images of cross-section morphologies in back-scattered electron (BSE) mode. Immersion test was conducted out in the box-type resistance furnace (SX-8-10). The coated specimens were immersed in molten zinc at temperatures of 460±5 °C, and graphite crucible was used as a container for molten zinc. All the specimens were immersed for 360 h for the corrosion mechanism analysis.

The morphologies of powders and the cross-sectional microstructure of the coatings before and after corrosion were investigated using SEM (VEGA II-LSU, TESCAN, Czech Republic) equipped with energy dispersive spectroscopy (EDS) in BSE mode. The cross-sections of all specimens cold-mounted by polyester resin were ground using SiC abrasive paper of 800#, and then polished using diamond suspension of 0.25 μm. X-ray diffraction (XRD) analyses of the powders and the coatings were conducted using a Bruker-D8 advance diffractometer (Karlsruhe, Germany). The XRD analysis was conducted using Cu Kα (λ=0.154 18 nm) radiation with 2θ= 20°~90°.

2 Results and Discussion

2.1 Microstructure of Mo-B-Ni-Cr mixture powders

Fig. 2 shows the surface and cross-sectional morphologies of Mo-B-Ni-Cr mixture powders with different (Mo+B)/(Ni+Cr) mass ratios of 1:1, 2:1, and 3:1. As shown in Fig. 2a~2c, Mo, B, Ni, and Cr particles are combined with each other to form the Mo-B-Ni-Cr mixture powders under the effect of PVA binder. In addition, the morphologies of three kinds of the mixture powders present nearly spherical shape, which is beneficial to the fluidity of HVOF spraying process. Compared with the original materials (Fig. 1), it can be obviously seen that Mo, B, Ni, and Cr particles deform and form the finer particles after ball milling (Fig. 2d~2f) owing to the impacting effect. The size distribution (D_{50}) of three kinds of Mo-B-Ni-Cr mixture powders is 30.5, 31.3, and 32.3 μm. XRD patterns of Mo-B-Ni-Cr mixture powders (Fig. 3) indicate that the main phase composition of all coatings is Mo, Ni, and Cr phases. It also reveals that due to the protection effect of anhydrous ethanol and pure argon, no oxidation or phase transformation occurs during ball milling. Besides, with increasing the (Mo+B)/(Ni+Cr) mass ratio of Mo-B-Ni-Cr mixture powders, the intensity of Mo phase is increased, while that of Ni and Cr phases is decreased.

2.2 XRD patterns of MoB/NiCr coatings

Fig. 4 shows XRD patterns of the in situ synthesized MoB/NiCr coatings with different (Mo+B)/(Ni+Cr) mass ratios (1:1, 2:1, and 3:1). It indicates that the main phases of all as-

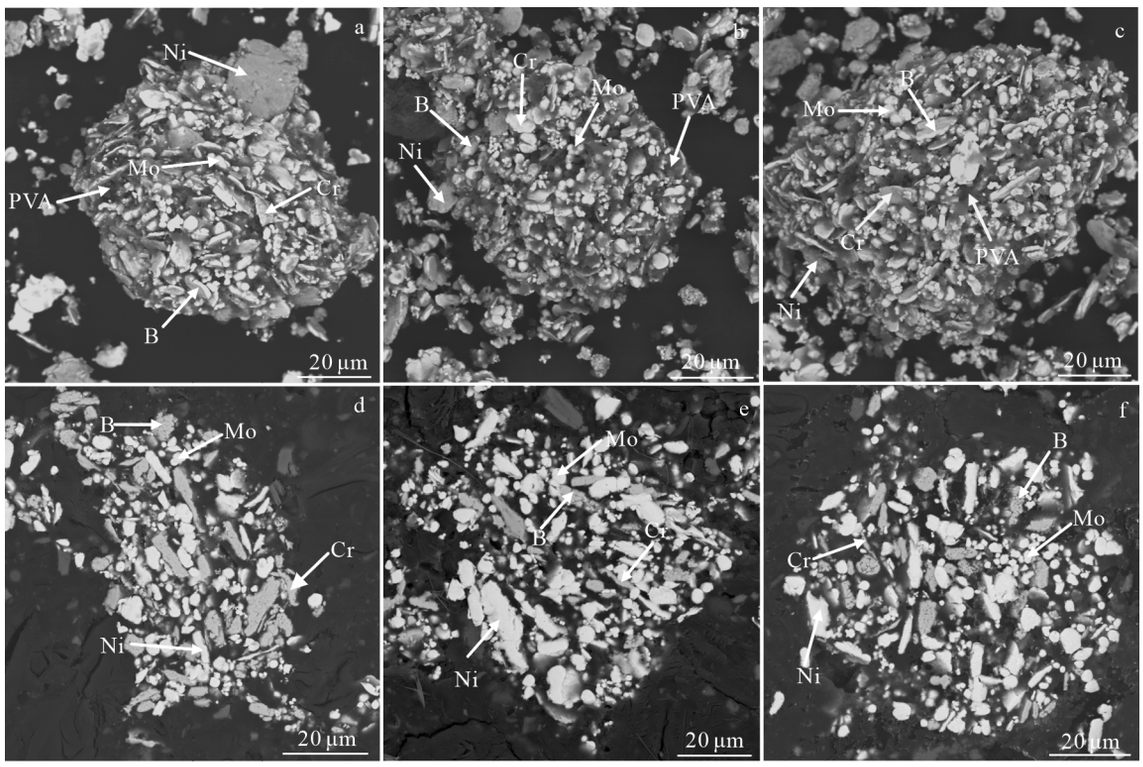

Fig. 2 Surface (a~c) and cross-section (d~f) morphologies of Mo-B-Ni-Cr mixture powders with (Mo+B)/(Ni+Cr) mass ratios of 1:1 (a, d), 2:1 (b, e), and 3:1 (c, f)

sprayed MoB/NiCr coating consist of Mo_2NiB_2 and Ni phases, and other phases, such as Mo, Cr, Cr_2O_3, and NiO phases can be detected as well. This result reveals that Mo_2NiB_2 ternary boride can be in situ synthesized in the coatings during spraying owing to the elevated temperature effect, while some original phases (Mo, Cr, and Ni) which do not react with other phases remain. Some oxides (Cr_2O_3 and NiO) are formed in all the coatings. In addition, with increasing the (Mo+B)/(Ni+Cr) mass ratio of Mo-B-Ni-Cr mixture powders, the intensity of Mo_2NiB_2 ternary boride is increased, while that of Ni and Cr is decreased. This phenomenon illustrates that the increase in (Mo+B)/(Ni+Cr) mass ratio is beneficial to improving the reaction probability of spraying particles, thereby increasing the content of Mo_2NiB_2 ternary boride in the coating.

2.3 Microstructure of MoB/NiCr coatings

Fig. 5 shows the SEM-BSE images of cross-sectional morphologies of MoB/NiCr coatings. Due to the melted Mo-B-Ni-Cr particles impacting on the substrate at elevated temperature and high velocity, the flattening of the particles occurs. Thus, the typical lamellar structure of MoB/NiCr coatings can be observed, as shown in Fig. 5b, 5d, and 5f. Furthermore, there are no obvious micro-cracks among the phases in the MoB/NiCr coatings or between the MoB/NiCr coating and Co-based alloy coating, or between the Co-based alloy coating and substrate, as shown in Fig.5a, 5c, and 5e. In order to analyze the composition of MoB/NiCr coatings after HVOF spraying, the phase composition was analyzed by EDS. The results of chemical composition analyses of points

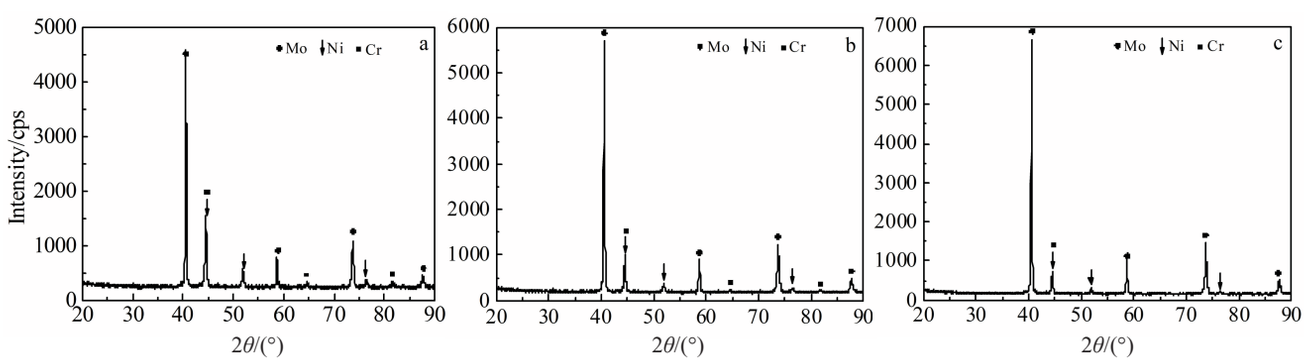

Fig.3 XRD patterns of Mo-B-Ni-Cr mixture powders with (Mo+B)/(Ni+Cr) mass ratios of 1:1 (a), 2:1 (b), and 3:1 (c)

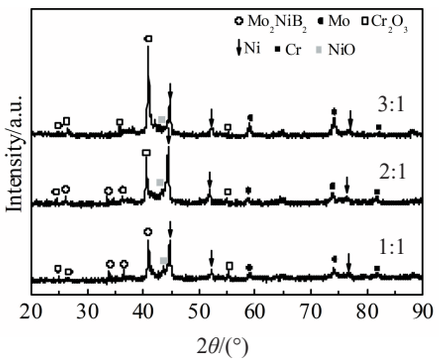

Fig.4 XRD patterns of MoB/NiCr coatings with different (Mo+B)/(Ni+Cr) mass ratios

marked in Fig. 5b, 5d, and 5f are listed in Tables 2, 3, and 4, respectively. According to XRD patterns in Fig. 4, EDS analysis reveals that Mo_2NiB_2 ternary boride phase (point 1 in Fig. 5b, 5d, and 5f) is generated in the MoB/NiCr coatings. Meanwhile, the original pure Mo (point 2), Ni (point 4), and Cr (point 6) remain, and Cr_2O_3 (point 3) and NiO (point 5) oxides are generated in the coatings, as shown in Fig. 5b, 5d, and 5f. This analysis result also further confirms that Mo_2NiB_2 ternary boride is in situ synthesized in the coatings.

The average porosities of MoB/NiCr coatings with different (Mo+B)/(Ni+Cr) mass ratios of 1:1, 2:1, and 3:1 are 0.313%, 1.04%, and 1.25%, respectively, which illustrates that MoB/NiCr coating with (Mo+B)/(Ni+Cr) mass ratio of 1:1 has the densest structure among the coatings. The reason for this phenomenon is that the content of Ni and Cr metal phases in the coating with (Mo+B)/(Ni+Cr) mass ratio of 1:1 is more than that of the other two coatings. Thus, the probability of filling pores by melted metal phases is greater. Furthermore, it is difficult for the subsequent impacting particles with lower content of metal phase to completely fill the pores, because of the cooling shrinkage and rebounding-off of Mo_2NiB_2 ternary boride. Therefore, it leads to the increase of porosity in the coating. The average content of Mo_2NiB_2 ternary boride in MoB/NiCr coatings of different (Mo+B)/(Ni+Cr) mass ratios of 1:1, 2:1, and 3:1 is 44.08vol%±1.60vol%, 51.39vol%±0.72vol%, and 54.81vol%±0.76vol%, respectively, confirming that with increasing the (Mo+B)/(Ni+Cr) mass ratio, the content of Mo_2NiB_2 ternary boride in the coating is increased. This analysis result is completely consistent with XRD analysis of the coatings. Therefore, due to the highest Mo_2NiB_2 ternary boride content in MoB/NiCr coating with (Mo+B)/(Ni+Cr) mass ratio of 3:1, the influence of cooling shrinkage and rebounding-off of ternary boride for the coating is more serious, which leads to the highest porosity for the coating. Meanwhile, the rebounding-off of spraying particles can reduce the thickness of the coating under the same spraying conditions. Therefore, the average thickness of MoB/NiCr coatings with different (Mo+B)/(Ni+Cr) mass ratios of 1:1, 2:1, and 3:1 is 282.10±20.33, 221.33±15.64, and 198.94±29.71 μm, respectively.

2.4 Microhardness and bond strength of MoB/NiCr coatings

The average microhardness ($HV_{0.3}$) of MoB/NiCr coatings

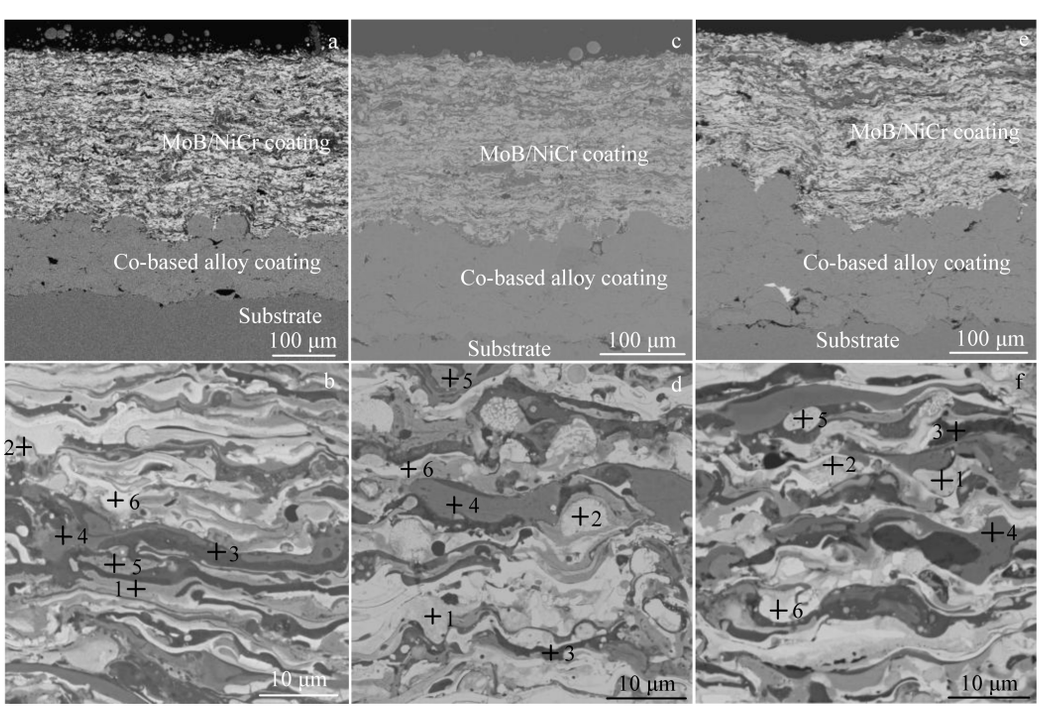

Fig.5 SEM-BSE images (a, c, e) and magnified images (b, d, f) of cross-sectional morphologies of MoB/NiCr coating with (Mo+B)/(Ni+Cr) mass ratios of 1:1 (a, b), 2:1 (c, d), and 3:1 (e, f)

Table 2 EDS results of chemical composition of points 1~6 in Fig.5b (at%)

Point	Mo	Ni	Cr	O	Phase
1	65.31	34.69	0.00	0.00	Mo_2NiB_2
2	94.13	5.87	0.00	0.00	Mo
3	0.00	0.00	47.60	52.40	Cr_2O_3
4	0.00	100.00	0.00	0.00	Ni
5	0.00	50.49	0.00	49.51	NiO
6	0.00	0.00	100.00	0.00	Cr

Table 3 EDS results of chemical composition of points 1~6 in Fig.5d (at%)

Point	Mo	Ni	Cr	O	Phase
1	64.09	35.91	0.00	0.00	Mo_2NiB_2
2	100.00	0.00	0.00	0.00	Mo
3	0.00	0.00	44.97	55.03	Cr_2O_3
4	0.00	100.00	0.00	0.00	Ni
5	0.00	49.53	0.00	50.47	NiO
6	0.00	0.00	100.00	0.00	Cr

Table 4 EDS result of chemical composition of points 1~6 in Fig.5f (at%)

Point	Mo	Ni	Cr	O	Phase
1	68.32	31.68	0.00	0.00	Mo_2NiB_2
2	100.00	0.00	0.00	0.00	Mo
3	0.00	0.00	48.79	51.21	Cr_2O_3
4	0.00	100.00	0.00	0.00	Ni
5	0.00	48.58	0.00	51.42	NiO
6	0.00	0.00	100.00	0.00	Cr

with different (Mo+B)/(Ni+Cr) mass ratios of 1∶1, 2∶1, and 3∶1, Co-based coating, and 316L stainless-steel substrate is 6381±104, 6711±205, 7338±219, 4013±311, and 2511±213 MPa, respectively. It can be seen that the microhardness of all MoB/NiCr coatings is obviously higher than that of the substrate, and the microhardness of MoB/NiCr coatings with (Mo+B)/(Ni+Cr) mass ratio of 3∶1 is about 3 times higher than that of the substrate. Furthermore, with increasing the (Mo+B)/(Ni+Cr) mass ratio, the microhardness of MoB/NiCr coatings is gradually increased. Therefore, MoB/NiCr coating with (Mo+B)/(Ni+Cr) mass ratio of 3∶1 has the highest microhardness value. Guo[18] and Yan[19] et al reported that according to the mixture principle of composites, an addition of hard phase in a soft matrix can increase the microhardness of the materials. Hou et al[20] also reported that the microhardness of the coatings is related to the content of boride ceramics, and the addition of boride ceramics, as a particulate reinforcement, increases the microhardness of the coating. Mizuno[6] and Moghaddam[21] et al reported that the presence of ternary boride phases in the coatings can increase the microhardness. Therefore, the in situ synthesized Mo_2NiB_2 ternary boride can increase the microhardness of the coating, and the microhardness is increased with increasing the ternary boride content in this study.

Bond strength directly related to the coating durability is one of the most important factors in thermal spray coating[22-25]. In this study, the bond strength of MoB/NiCr coatings with different (Mo+B)/(Ni+Cr) mass ratios of 1∶1, 2∶1, and 3∶1 is 63.93±1.95, 56.88±0.71, and 49.23±1.67 MPa, respectively. The bond strength values of MoB/NiCr coatings are decreased with increasing the (Mo+B)/(Ni+Cr) mass ratio. Zhang et al[26] revealed that although the microhardness of the coating is improved by the increase in the content of ceramic-reinforcing phase, incomplete contact between the ceramic sheets may occur owing to the higher porosity of the coating, which leads to reduction of the bond strength of the coating. Therefore, due to the highest porosity of MoB/NiCr coating of (Mo+B)/(Ni+Cr) mass ratio of 3∶1, there are many pores in the interface of Mo_2NiB_2 ternary boride, which decreases the bond strength of the coating in this study. The adhesive strength of the coating is increased with increasing the roughness of the substrate surface[27-30]. In this study, the average surface roughness of Co-based alloy bond coating (6.48±0.36 μm) is higher than that of 316L stainless-steel substrate (2.41±0.57 μm). Therefore, due to the Co-based alloy bond coating, the bond strength values of three kinds of coatings in this study are higher than that of MoB/NiCr coating directly deposited on the substrate surface (46.99±1.20 MPa).

2.5 Corrosion behavior of MoB/NiCr coatings

Fig.6~Fig.8 show SEM images and EDS analyses of MoB/NiCr coatings with different (Mo+B)/(Ni+Cr) mass ratios of 1∶1, 2∶1, and 3∶1 immersed in the molten zinc at 460 °C for 360 h, respectively. Fig. 6b, Fig. 7b, and Fig. 8b show SEM images and EDS line scanning analyses of the black square in Fig. 6a, Fig. 7a, and Fig. 8a, respectively. Meanwhile, the related EDS line scanning results of element O, Cr, Ni, Mo are shown in Fig. 6c, Fig. 7c, and Fig. 8c. No obvious vertical micro-cracks are generated between the MoB/NiCr coating and Co-based alloy coating or between the Co-based alloy coating and the substrate (as shown in Fig. 6a, Fig. 7a, and Fig. 8a). Furthermore, due to the Mo_2NiB_2 ternary boride with excellent durability and the hindrance effect of the lamellar microstructure of MoB/NiCr coating[6,15-17], no zinc element or its intermetallic compound can be observed in the surface region of MoB/NiCr coatings (as indicated by Fig. 6b, Fig. 7b, and Fig. 8b) according to the results of EDS and XRD analyses (as shown in Fig. 9). Meanwhile, the phase composition of MoB/NiCr coatings after immersion test is similar to that of the coatings before immersion (as shown in Fig. 4). However, compared with MoB/NiCr coatings before corrosion, the average porosity of three kinds of MoB/NiCr coatings is increased after immersion test, especially that of the MoB/NiCr coating of (Mo+B)/(Ni+Cr) mass ratio of 3∶1. The average porosity of MoB/NiCr coatings with different (Mo+B)/(Ni+Cr) mass ratios of 1∶1, 2∶1, and 3∶1 after immersion test is 1.15%, 1.86%, and 12.57%, respectively. Meanwhile, the thickness of MoB/NiCr coatings with different (Mo+B)/(Ni+Cr) mass ratios of 1∶1, 2∶1, and 3∶1 after immersion test is

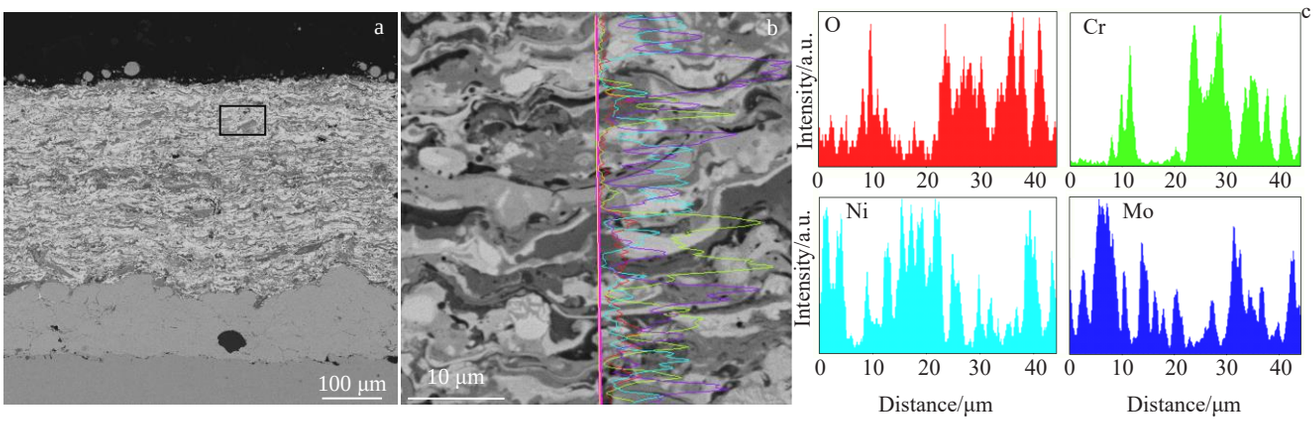

Fig.6 SEM image (a); EDS line scanning result of corresponding black square (b); EDS line scanning of element O, Cr, Ni, Mo (c) for MoB/NiCr coating with (Mo+B)/(Ni+Cr) mass ratio of 1:1 after immersion test in molten zinc at 460 °C for 360 h

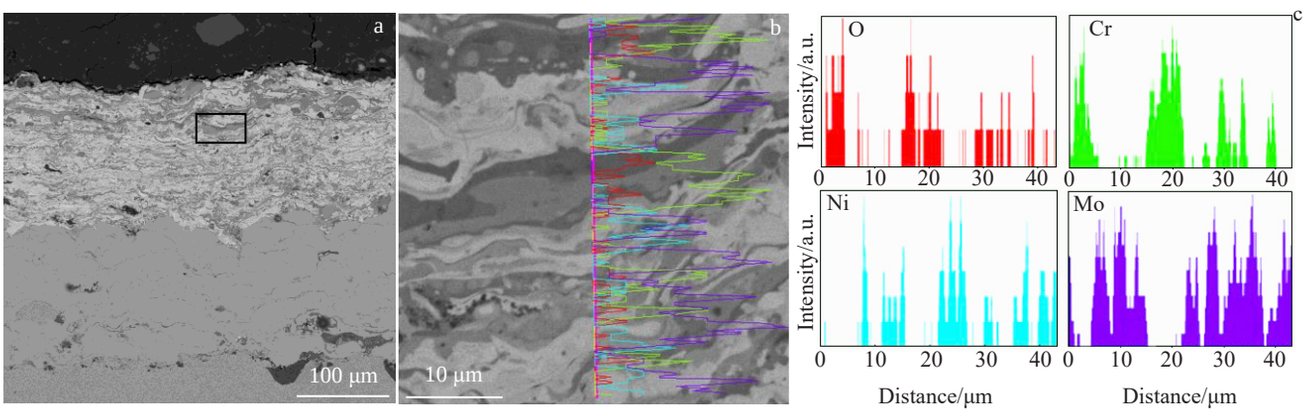

Fig.7 SEM image (a); EDS line scanning result of corresponding black square (b); EDS line scanning of element O, Cr, Ni, Mo (c) for MoB/NiCr coating with (Mo+B)/(Ni+Cr) mass ratio of 2:1 after immersion test in molten zinc at 460 °C for 360 h

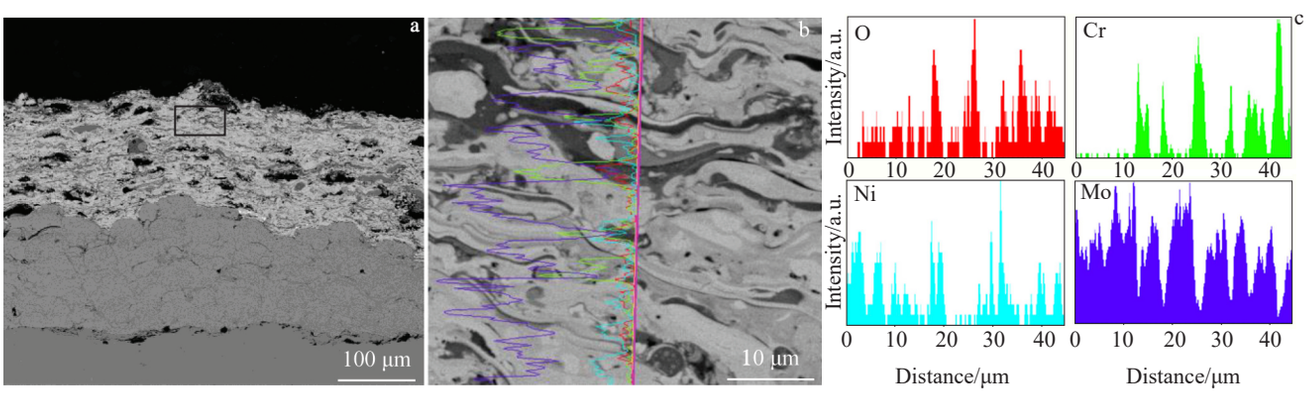

Fig.8 SEM image (a); EDS line scanning result of corresponding black square (b); EDS line scanning of element O, Cr, Ni, Mo (c) of MoB/NiCr coating with (Mo+B)/(Ni+Cr) mass ratio of 3:1 after immersion test in molten zinc at 460 °C for 360 h

278.40±21.43, 171.95±12.42, and 163.45±23.59 μm, respectively. The reasons for these phenomena are that the cracks (as shown in Fig. 10) are generated between the weak interfacial bonding phases in the coating. Hence, the pores in the coating increase, and the peel-off phenomenon occurs, leading to the decrease of the thickness of the coating. Therefore, due to the highest porosity and the weakest interfacial bonding of MoB/NiCr coating with (Mo+B)/(Ni+Cr) mass ratio of 3:1 before

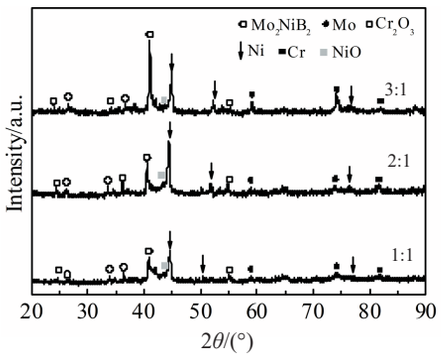

Fig.9 XRD patterns of MoB/NiCr coatings with different (Mo+B)/(Ni+Cr) mass ratios after immersion test in molten zinc at 460 °C for 360 h

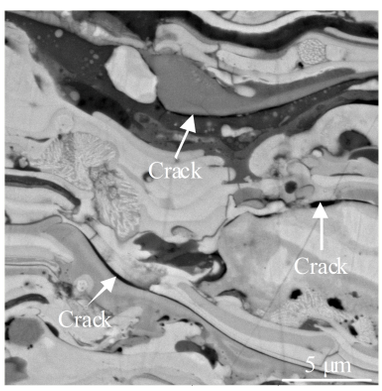

Fig.10 Cross-sectional morphology of MoB/NiCr coating with (Mo+B)/(Ni+Cr) mass ratio of 3:1 after immersion test in molten zinc at 460 °C for 360 h

corrosion, the highest increment of the porosity and the fastest decrease of the thickness appear in this coating during immersion test.

3 Conclusions

1) The morphologies of Mo-B-Ni-Cr mixture powders with different (Mo+B)/(Ni+Cr) mass ratios of 1:1, 2:1, and 3:1 present nearly spherical shape. The size distribution (D_{50}) of three kinds of Mo-B-Ni-Cr mixture powders is 30.5, 31.3, and 32.3 μm, respectively. The main phase composition of Mo-B-Ni-Cr mixture powders are Mo, Ni, and Cr phases. With increasing the (Mo+B)/(Ni+Cr) mass ratio of Mo-B-Ni-Cr mixture powders, the intensity of Mo phase is increased, while that of Ni and Cr phases is decreased.

2) The average porosities of MoB/NiCr coatings with different (Mo+B)/(Ni+Cr) mass ratios of 1:1, 2:1, and 3:1 are 0.313%, 1.04%, and 1.25%, respectively. The average thickness of MoB/NiCr coatings with different (Mo+B)/(Ni+Cr) mass ratios of 1:1, 2:1, and 3:1 is 282.10±20.33, 221.33±15.64, and 198.94±29.71 μm, respectively. Based on XRD and EDS results, Mo_2NiB_2 ternary boride is in situ synthesized in all MoB/NiCr coatings. The average ternary boride contents of MoB/NiCr coatings with different (Mo+B)/(Ni+Cr) mass ratios of 1:1, 2:1, and 3:1 are 44.08vol% ±1.60vol% , 51.39vol%±0.72vol%, and 54.81vol%±0.76vol%, respectively.

3) The microhardness ($HV_{0.3}$) of MoB/NiCr coating with (Mo+B)/(Ni+Cr) mass ratio of 3:1 (7338±219 MPa) is about 3 times higher than that of the substrate (2511±213 MPa). Due to the influence of the porosity on the coating, the bond strength of MoB/NiCr coatings is decreased with increasing the (Mo+B)/(Ni+Cr) mass ratio. MoB/NiCr coating with (Mo+B)/(Ni+Cr) mass ratio of 3:1 has the lowest bond strength.

4) Due to the highest porosity and the weakest interfacial bonding, the highest increment of the porosity and the fastest decrease of the thickness appear in MoB/NiCr coating with (Mo+B)/(Ni+Cr) mass ratio of 3:1 during immersion test.

References

1 Sirin S Y. *International Journal of Fatigue*[J], 2019, 123: 1
2 Shibli S M A, Meena B N, Remya R. *Surface & Coatings Technology*[J], 2015, 262(1): 210
3 Chang J K, Lin C S, Cheng W J *et al. Corrosion Science*[J], 2020, 164: 108 307
4 Peng B C, Wang J H, Su X P *et al. Surface & Coatings Technology*[J], 2008, 202(9): 1785
5 Matthews S, James B. *Journal of Thermal Spray Technology*[J], 2010, 19(6): 1277
6 Mizuno H, Kitamura J. *Journal of Thermal Spray Technology*[J], 2007, 16(3): 404
7 Seong B G, Hwang S Y, Kim M C *et al. Surface & Coatings Technology*[J], 2001, 138(1): 101
8 Zhang J F, Deng C M, Song J B *et al. Surface & Coatings Technology*[J], 2013, 235: 811
9 Xie X L, Yin F C, Wang X M *et al. Journal of Thermal Spray Technology*[J], 2019, 28(6): 1252
10 Dong Y C, Yan D R, He J N *et al. Surface & Coatings Technology*[J], 2006, 201(6): 2455
11 Yan D R, Yang Y, Dong Y C *et al. Intermetallics*[J], 2012, 22: 160
12 Ptačinová J, Drienovský M, Palcut M *et al. Kovove Materialy*[J], 2015, 53(3): 175
13 Takagi K, Koike W, Momozawa A *et al. Solid State Sciences*[J], 2012, 14(11-12): 1643
14 Wei X, Chen Z G, Zhong J *et al. Surface & Coatings Technology* [J], 2016, 296: 58
15 Lv H P, Wang J, Yan Y G *et al. Materials Science and Technology*[J], 2010, 26(8): 950
16 Lv H P, Nie P L, Yan Y G *et al. Journal of Coatings Technology and Research*[J], 2010, 7(6): 801
17 Khan F F, Bae G, Kang K *et al. Journal of Thermal Spray Technology*[J], 2011, 20(5): 1022
18 Guo B G, Zhou J S, Zhang S T *et al. Materials Science and Engineering A*[J], 2008, 480(1-2): 404

19 Yan H, Zhang P L, Yu Z S *et al. Surface & Coatings Technology* [J], 2012, 206(19-20): 4046
20 Hou S X, Liu Z D, Liu D Y. *Surface & Coatings Technology*[J], 2011, 205(19): 4562
21 Moghaddam S R, Kaya F, Derin B. *Engineering Science and Technology, an International Journal*[J], 2019, 22(6): 1193
22 Wang Y Y, Li C J, Ohmori A. *Surface & Coatings Technology*[J], 2006, 200(9): 2923
23 Loghman-Estarki M R, Hajizadeh-Oghaz M, Edris H *et al. Ceramics International*[J], 2018, 44(11): 12 042
24 Gu L J, Fan X Z, Zhao Y *et al. Surface & Coatings Technology* [J], 2012, 206(21): 4403
25 Inagaki M, Yokogawa Y, Kameyama T. *Surface & Coatings Technology*[J], 2003, 173(1): 1
26 Zhang W C, Liu L B, Zhang M T *et al. Transactions of Nonferrous Metals Society of China*[J], 2015, 25(11): 3700
27 Lin L, Li G L, Wang H D *et al. Applied Surface Science*[J], 2015, 356(30): 383
28 Cho T Y, Yoon J H, Cho J Y *et al. Surface & Coatings Technology*[J], 2009, 203(20-21): 3250
29 Wang Y Y, Li C J, Ohmori A. *Thin Solid Films*[J], 2005, 485(1-2): 141
30 Li C J, Wang Y Y, Wu T *et al. Surface & Coatings Technology* [J], 2001, 145(1-3): 113

不同(Mo+B)/(Ni+Cr)质量比的原位合成MoB/NiCr涂层的组织结构与性能

陈　枭[1,3]，李承娣[1,2]，周鸿凯[1]，皮智敏[1]，白小波[3]
(1. 新余学院 新余市智能制造材料技术与应用重点实验室，江西 新余 338004)
(2. 大连海事大学 海底工程技术与装备国际联合研究中心，辽宁 大连 116026)
(3. 九江学院 江西省表面绿色再制造工程技术中心，江西 九江 332005)

摘　要：采用超音速火焰喷涂技术沉积含3种不同(Mo+B)/(Ni+Cr)质量比（1:1，2:1和3:1）的Mo-B-Ni-Cr球磨复合粉末以原位反应制备获得MoB/NiCr涂层。采用扫描电子显微镜（SEM）和X射线衍射仪（XRD）分析了MoB/NiCr涂层的组织结构和物相。同时讨论了不同(Mo+B)/(Ni+Cr)质量比对涂层的组织结构、硬度、结合强度和耐腐蚀性能的影响。研究结果表明，(Mo+B)/(Ni+Cr)质量比为1：1的MoB/NiCr涂层孔隙率最低及涂层厚度最大。在3种涂层中均原位反应生成了Mo_2NiB_2三元硼化物，且随着(Mo+B)/(Ni+Cr)质量比的增加，涂层中三元硼化物含量随之增加，涂层的硬度值增加，结合强度反而随之降低；由于涂层中三元硼化物的原位生成，MoB/NiCr涂层的硬度值均高于316L不锈钢基体。通过能谱和XRD分析发现，经过360 h熔融锌腐蚀试验后，涂层表层中没有发现锌元素及其金属间化合物，然而随着(Mo+B)/(Ni+Cr)质量比的增加，涂层的孔隙率增加及厚度降低。最后，综合分析可得，相比其他涂层，(Mo+B)/(Ni+Cr)质量比为1:1的MoB/NiCr涂层具有更好的耐熔融锌腐蚀能力。

关键词：Mo_2NiB_2三元硼化物；超音速火焰喷涂；组织结构；硬度；耐腐蚀

作者简介：陈　枭，男，1984年生，博士，副教授，新余学院机电工程学院，江西 新余 338004，电话：0790-6666108，E-mail：chenxiaoxyxy@126.com